



HAL
open science

Parametric instabilities in modulated fiber ring cavities

Matteo Conforti, François Copie, Arnaud Mussot, Alexandre Kudlinski,
Stefano Trillo

► **To cite this version:**

Matteo Conforti, François Copie, Arnaud Mussot, Alexandre Kudlinski, Stefano Trillo. Parametric instabilities in modulated fiber ring cavities. *Optics Letters*, 2016, 41 (21), pp.5027-5030. 10.1364/OL.41.005027 . hal-02387264

HAL Id: hal-02387264

<https://hal.science/hal-02387264>

Submitted on 29 Nov 2019

HAL is a multi-disciplinary open access archive for the deposit and dissemination of scientific research documents, whether they are published or not. The documents may come from teaching and research institutions in France or abroad, or from public or private research centers.

L'archive ouverte pluridisciplinaire **HAL**, est destinée au dépôt et à la diffusion de documents scientifiques de niveau recherche, publiés ou non, émanant des établissements d'enseignement et de recherche français ou étrangers, des laboratoires publics ou privés.

Parametric instabilities in modulated fiber ring cavities

Matteo Conforti, François Copie, Arnaud Mussot, Alexandre Kudlinski,
Stefano Trillo

► **To cite this version:**

Matteo Conforti, François Copie, Arnaud Mussot, Alexandre Kudlinski, Stefano Trillo. Parametric instabilities in modulated fiber ring cavities. *Optics Letters*, Optical Society of America, 2016, 41 (21), pp.5027. 10.1364/OL.41.005027 . hal-02387264

HAL Id: hal-02387264

<https://hal.archives-ouvertes.fr/hal-02387264>

Submitted on 29 Nov 2019

HAL is a multi-disciplinary open access archive for the deposit and dissemination of scientific research documents, whether they are published or not. The documents may come from teaching and research institutions in France or abroad, or from public or private research centers.

L'archive ouverte pluridisciplinaire **HAL**, est destinée au dépôt et à la diffusion de documents scientifiques de niveau recherche, publiés ou non, émanant des établissements d'enseignement et de recherche français ou étrangers, des laboratoires publics ou privés.

Parametric instabilities in modulated fiber ring cavities

MATTEO CONFORTI^{1,*}, FRANÇOIS COPIE¹, ARNAUD MUSSOT¹, ALEXANDRE KUDLINSKI¹, AND STEFANO TRILLO²

¹Univ. Lille, CNRS, UMR 8523 - PhLAM - Physique des Lasers Atomes et Molécules, F-59000 Lille, France

²Department of Engineering, University of Ferrara, Via Saragat, 44122 Ferrara, Italy

*matteo.conforti@univ-lille1.fr

Compiled September 22, 2016

We investigate modulational instability in inhomogeneous passive cavities modeled by the Ikeda map. The cavity boundary conditions and the modulation of the fiber dispersion force the system to develop parametric instabilities, which lead to the generation of simple as well as period doubled temporal patterns. The analytical results obtained by means of Floquet theory are validated through numerical solution of the Ikeda map, and the limitation of the mean-field Lugiato-Lefever model are highlighted.

OCIS codes:

<http://dx.doi.org/10.1364/ol.XX.XXXXXX>

Instabilities in passive optical cavities [1–4] have a wealth of applications ranging from spatial pattern formation to generations of individually addressable solitons, pulse trains, and frequency combs. A central mechanism behind such applications is modulational instability (MI), the growth of sideband pairs due to underlying phase-matched four-photon processes in the cavity [4–8]. MI plays a crucial role in the dynamics of both fiber-based cavities and microresonators [9]. A mean field approach allows for a universal description of such phenomenon in terms of the so-called Lugiato-Lefever equation (LLE) [4–7]. In this framework, it has been predicted that the domain of cavity MI can be significantly extended by means of a periodic modulation of one or more cavity parameters such as GVD [10], nonlinearity [11], or losses [12]. In particular, such periodic driving leads to the onset of parametric resonances [13], which are responsible for additional new branches of MI, interpretable also in terms of quasi-phase-matching arguments. The latter, however, give only a zero-order description of the process [14]. Such narrowband MI branches, usually known as Arnold tongues are characteristic of the general class of Faraday instabilities (see, e.g. [15]) sustained by periodic driving, as opposed to Turing-type MI, which exist in the absence of periodic variations of the parameters. The competition between Turing-type and Faraday-type branches have been recently observed in a fiber resonator with average normal GVD [16]. At variance with free-running propagation, where periodic GVD is responsible for MI also in the normal GVD regime [14, 17–23], in the cavity what is observed is the cross-over between a Turing-type MI existing also without GVD modulation [5, 6] and new para-

metric Faraday-type branches due to the periodic GVD.

However, a different kind of parametric instability occurs even in *homogeneous* passive cavities, owing to the intrinsic periodicity associated with the cavity boundary conditions [3, 24–27]. This type of instability can only be predicted on the basis of the full Ikeda map [3, 6, 24]. This leads to a MI with period doubling (P2) features, which have been first observed in [24].

In this letter, we investigate the competition of this type of parametric instability with those due to the presence of a periodic GVD. We extend the analytical approach of [3, 24], which allows us to assess the physically different character of the various branches of parametric instability. We find that the branches induced by the periodic-GVD extend and enhance the ones generated by the cavity boundary conditions. Moreover, we highlight the general limitation of the LLE approach proposed in [10]. Such analysis is crucial in order to experimentally explore new regimes in modulated fiber cavities, and more generally, to understand the limit of validity of averaged descriptions to account for the observed dynamics [27, 28].

We consider a fiber ring modeled by cavity boundary conditions for the n -th round-trip, coupled to Nonlinear Schrödinger Equation (NLSE), that rules the propagation of the intracavity field u_n along the n -th circulation along the ring:

$$u_{n+1}(z=0, t) = \theta u_{in}(t) + \rho e^{i\phi_0} u_n(z=1, t), \quad (1)$$

$$i \frac{\partial u_n}{\partial z} - \frac{\beta(z)}{2} \frac{\partial^2 u_n}{\partial t^2} + |u_n|^2 u_n = 0, \quad (2)$$

where ρ, θ ($\rho^2 + \theta^2 = 1$) are the reflection and transmission coefficients, and ϕ_0 is the linear phase acquired by the field during one roundtrip. The dimensionless quantities in Eqs. (1–2) follow from scaling the distance in units of cavity length L , i.e. $z = Z/L$, $t = T/T_0$, $u(z, t) = E(Z, T)\sqrt{\gamma L}$, $u_{in}(t) = E_{in}(T)\sqrt{\gamma L}$, $T_0 = \sqrt{|k''|L}$, $\beta(z) = k''(z)/|k''|$, $k'' = d^2k/d\omega^2$ and γ being the average second order dispersion and the fiber nonlinearity, respectively. Quantities in capital letters Z, T, E, E_{in} denotes real world distance, retarded time in the frame traveling at group velocity, and intracavity and input electric field envelope, respectively.

We consider a steady state, continuous wave (cw) solution of Eq. (2): $u_n(z, t) = \sqrt{P} \exp(iPz)$, where the normalized intracavity power is related to the input power $P_{in} = |u_{in}|^2$ through the cavity steady state response: $P[1 + \rho^2 - 2 \cos(\phi_0 + P)] = \theta^2 P_{in}$. The stability of the cw solution is analyzed by insert-

ing the Ansatz $u_n(z, t) = [\sqrt{P} + \tilde{a}_n(z, t) + i\tilde{b}_n(z, t)] \exp(iPz)$ in Eq. (2), where \tilde{a}, \tilde{b} are small real perturbations. After linearization around the stationary solution, we get the system $d/dz[a_n, b_n]^T = M[a_n, b_n]^T$, ruling the evolution of the Fourier transform of the perturbations $[a_n(z, \omega), b_n(z, \omega)] = \mathcal{F}\{\tilde{a}_n(z, t), \tilde{b}_n(z, t)\}$, where

$$M(z) = \begin{bmatrix} 0 & -\frac{\beta(z)\omega^2}{2} \\ \frac{\beta(z)\omega^2}{2} + 2P & 0 \end{bmatrix}. \quad (3)$$

We recall first the theory for a homogeneous cavity with constant GVD β [3, 24, 27], linking the outcome to the concept of parametric resonance [13]. For simplicity, we will discuss in details the case $\beta = 1$ (normal GVD), where the cavity dynamics presents major qualitative differences with the cavity-less MI. The results can be trivially extended to the anomalous case $\beta = -1$. The fundamental matrix solution associated with Eq. (3) reads as

$$X(z) = \begin{bmatrix} \cos(kz) & -\frac{\beta\omega^2}{2k} \sin(kz) \\ \frac{2k}{\beta\omega^2} \sin(kz) & \cos(kz) \end{bmatrix}, \quad (4)$$

where $k = \sqrt{(\beta\omega^2/2 + 2P) \cdot \beta\omega^2/2}$ is the wavenumber shift of the perturbation (imaginary k gives the gain of the standard cavity-less MI, obtained only for $\beta < 0$). The perturbation at distance z is given, through Eq. (4), as $[a_n(z), b_n(z)]^T = X(z)[a_n(0), b_n(0)]^T$. Then, the boundary conditions (1) imposes that $[a_{n+1}(0), b_{n+1}(0)]^T = \Gamma[a_n(1), b_n(1)]^T$, where

$$\Gamma = \rho \begin{bmatrix} \cos(\phi) & -\sin(\phi) \\ \sin(\phi) & \cos(\phi) \end{bmatrix}, \quad (5)$$

where $\phi = \phi_0 + P$ is the total (linear plus nonlinear) phase acquired during a round-trip.

The Floquet matrix for the perturbation, say $\Psi \equiv \Theta\Gamma$, is found as the product of the matrix $\Theta \equiv X(z_L)$, i.e. the matrix (4) evaluated at the round-trip $z = z_L = 1$, and the boundary condition matrix Γ in Eq. (5). The perturbation at the n -th round-trip evolves as $[a_n(0), b_n(0)]^T = \Psi^n[a_0(0), b_0(0)]^T$. Therefore the stability of the system is determined by the eigenvalues of matrix Ψ

$$\lambda_{\pm} = \Delta/2 \pm \sqrt{\Delta^2/4 - \rho^2}, \quad (6)$$

where $\Delta = \rho[2\cos(\phi)\cos(kz_L) - \frac{\beta\omega^2+2P}{k} \cdot \sin(\phi)\sin(kz_L)]$. Whenever $|\lambda_-|$ or $|\lambda_+|$ exceed unity, the cw solution is unstable and the perturbation grows as $\exp[g(\omega)z]$ with MI gain $g(\omega) = \ln(\max\{|\lambda_-(\omega)|, |\lambda_+(\omega)|\})$. This generally occurs for $|\Delta| > 1 + \rho^2$. In the good cavity limit ($\rho \simeq 1$), the threshold for instability $|\Delta| = 2$, assuming also moderate powers such that $(\beta\omega^2 + 2P)/k \simeq 2$, reads as

$$k + P + \phi_0 = m\pi, \quad m = 0, \pm 1, \pm 2, \dots \quad (7)$$

Returning to dimensional quantities, by introducing the frequency $\Omega = \omega T_0^{-1}$ and the wavenumber $K = kL^{-1} = \sqrt{(k''\Omega^2/2 + 2\gamma|E_0|^2) \cdot k''\Omega^2/2}$, we cast Eq. (7) in the form

$$K + \frac{\gamma|E_0|^2 L + \phi_0}{L} = m\frac{\pi}{L}, \quad m = 0, \pm 1, \pm 2, \dots \quad (8)$$

which is clearly interpretable, for $m \neq 0$, as a *parametric resonance* condition, where the overall perturbation wavenumber [the LHS in Eq. (8)] equals a multiple of the halved "driving"

wavenumber $2\pi/L$ associated with the round-trip periodicity [13]. The frequency of the m -th unstable band (within such approximations) is

$$\omega_m = \sqrt{\frac{2}{\beta}} \sqrt{\sqrt{(m\pi - P - \phi_0)^2 + P^2} - P}. \quad (9)$$

Next, we extend such an approach to an inhomogeneous cavity with GVD of normalized period $\Lambda = 1/N$, where the integer N stands for the number of periods contained over the cavity length. In particular we consider henceforth the piecewise constant case [16], where $\Lambda = z_A + z_B, z_{A,B}$ being the length of two fiber sections with different GVD $\beta_{A,B}$. In this case, the relevant eigenvalues are those of the overall Floquet matrix, calculated as the product

$$\Psi = (\Theta_A \Theta_B)^N \Gamma, \quad (10)$$

being Θ_A and Θ_B the fundamental matrix solution (4) for the fiber span A and B , calculated at z_A and z_B , respectively, and Γ the boundary condition matrix (5). When $N = 1$ (GVD periodic over the cavity length), we are still able to analytically obtain the eigenvalues in the form of Eq. (6), where the discriminant is now

$$\Delta = \rho \cos(\phi) [2\cos(k_A z_A) \cos(k_B z_B) - \sigma_1 \sin(k_A z_A) \sin(k_B z_B)] - \rho \sin(\phi) [\sigma_2 \sin(k_A z_A) \cos(k_B z_B) + \sigma_3 \cos(k_A z_A) \sin(k_B z_B)] \quad (11)$$

with

$$\sigma_1 = \frac{(\beta_A k_B)^2 + (\beta_B k_A)^2}{\beta_A \beta_B k_A k_B}, \quad \sigma_{2,3} = \frac{(\beta_{A,B} \omega^2)^2 + 4k_{A,B}^2}{2k_{A,B} \beta_{A,B} \omega^2}. \quad (12)$$

Expressions (11-12) constitute the main result of this Letter, which allows us to gain a full understanding of parametric resonances in cavities. Again, instability occurs for $|\Delta| > 1 + \rho^2$. Using the same approximations (good cavity, moderate powers) as above, we obtain that the instability threshold $|\Delta| = 2$ corresponds to the following parametric resonance condition

$$k_A z_A + k_B z_B + P + \phi_0 = m\pi, \quad m = 0, \pm 1, \pm 2, \dots \quad (13)$$

which suitably generalize Eq. (7) for an inhomogeneous cavity. The frequency of the unstable bands is still given by Eq. (9) with $\beta = \beta_{av} = (\beta_a z_a + \beta_b z_b)$ (for $N = 1$). For multiple periods of GVD over the cavity length ($N = 2, 3, \dots$) the analytical formulas become cumbersome but the unstable eigenvalues can be easily obtained numerically from the matrix Ψ in Eq. (10).

In order to compare with the LLE-based approach [4-6, 10, 16], we recall that the map (1-2) can be averaged to yield [6]

$$i\frac{\partial u}{\partial z} - \frac{\beta(z)}{2} \frac{\partial^2 u}{\partial t^2} + |u|^2 u = (\delta - i\alpha) u + iS, \quad (14)$$

where we drop the subscript n for the field and set $S = \theta u_{in}$, where $\alpha = 1 - \rho \approx \theta^2/2$ describes cavity losses (assuming the output coupling to dominate over fiber propagation loss), and the detuning is $\delta = -\phi_0$ (modulo 2π).

We briefly summarize the results of MI analysis in LLE with periodic GVD [10]. In the case of piecewise constant GVD with $N = 1$ (two fibers with GVD $\beta_{A,B}$ of length $z_{A,B}, z_A + z_B = 1$), the results are analytical and give the characteristic exponents, i.e. the eigenvalues of Ψ , as $\lambda_{\pm} = \frac{\Delta}{2} \pm \sqrt{\frac{\Delta^2}{4} - \exp[-2\alpha]}$. MI occurs if $|\Delta| > (1 + \exp[-2\alpha])$, where

$$\Delta = e^{-\alpha} [2\cos(k_A z_A) \cos(k_B z_B) - \sigma \sin(k_A z_A) \sin(k_B z_B)], \quad (15)$$

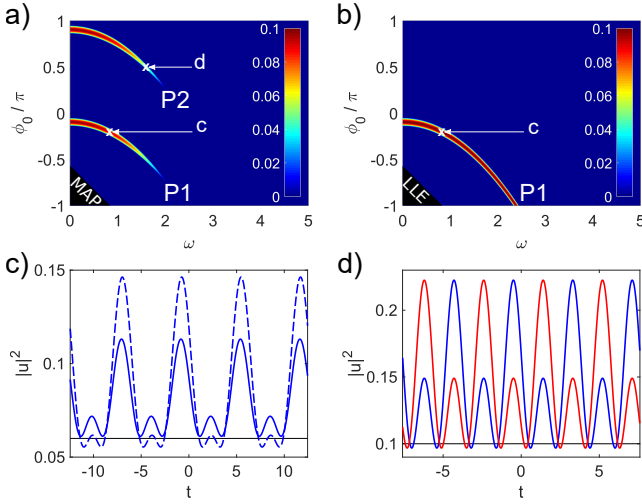


Fig. 1. (a), (b) Color level plot of gain $g(\omega)$ in the plane (ω, ϕ_0) of frequency and cavity linear shift (detuning), calculated from (a) Ikeda map and (b) LLE. Homogeneous cavity with normal GVD ($\beta = 1$), $P = 0.15$, $\alpha = \theta^2/2 = 0.05$. (c) P1 temporal profile from Ikeda map (solid curve) and LLE (dashed curve) for an intracavity power $P = 0.06$ and $\phi_0 = -\pi/5$, see white arrows in (a,b). (d) P2 pulse train from Ikeda map $P = 0.1$ and $\phi_0 = \pi/2$; red (blue) curves, even (odd) roundtrips

and $\sigma = [\beta_A \beta_B \omega^4 + 2(P - \delta)(\beta_A + \beta_B)\omega^2 + 4(3P - \delta)(P - \delta)] / (2k_A k_B)$, and $k_{A,B} = \sqrt{(\beta_{A,B}\omega^2/2 + 2P - \delta)^2 - P^2}$. An estimate of the central frequency of the m -th band is ($N = 1$)

$$\omega_m^{LLE} = \sqrt{\frac{2}{\beta_{av}} \left[\sqrt{(m\pi)^2 + P^2} + (\delta - 2P) \right]}. \quad (16)$$

We illustrate now some relevant examples, starting from a uniform cavity. Despite this case has been studied before [24, 27], some clarifications are needed. To this end, we plot in Fig. 1(a) the level plot of the parametric gain in a plane ω - ϕ_0 (perturbation frequency and cavity shift), obtained from the analysis of the map. One can notice two branches: the first one, labeled P1, is associated to the positive eigenvalue λ_+ and $m = 0$ in Eq. (7). It starts from zero frequency for quasi-resonant conditions $\phi_0 \approx 0$, and extend to higher frequencies as the phase shift ϕ_0 decreases towards negative values. This branch stands for the Turing-type MI, which is predicted also from the LLE [5, 6], as shown for comparison in Fig. 1(b). Conversely, the upper branch labeled P2, associated to λ_- , is located around $\omega = 0$ for anti-resonance conditions $\phi_0 \approx \pi$ and extend to higher frequencies as the cavity is brought towards resonance. This is a $m = 1$ parametric instability branch, which does not appear from the gain calculated from LLE, being due to the periodicity of the boundary conditions. This is consistent with the fact that LLE works only for small cavity detunings, and approximate the cavity transfer function (the Airy function) with a single Lorentzian. In both the P1 and P2 regimes, stable temporal patterns (pulse trains) can be generated at the maximally unstable ω . In the P1 regime, where the pulse train is equal at each round trip, the LLE and the map typically show only a small quantitative discrepancy in the attractive temporal periodic solutions, as shown in Fig. 1(c). However, the map additionally describes stable P2 regimes (at different phase-shift

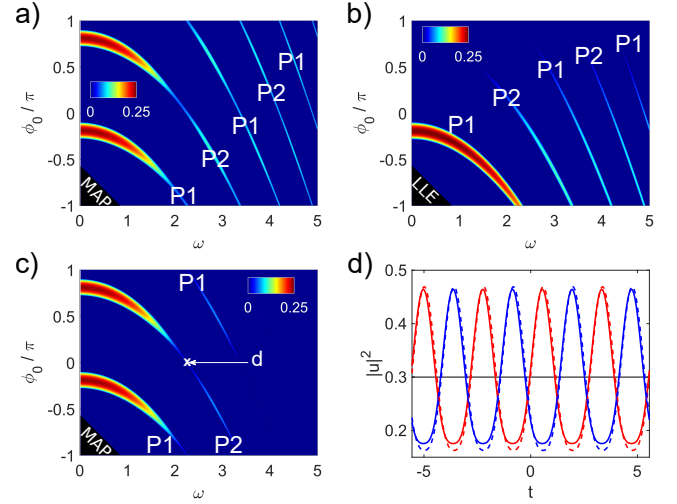


Fig. 2. (a), (b) Color level plot of gain $g(\omega)$ for an inhomogeneous cavity with $\beta_A = 1.9$, $\beta_B = 0.1$, $z_A = z_B = 0.5$, $P = 0.3$, $\alpha = \theta^2/2 = 0.05$ calculated from (a) Ikeda map and (b) LLE. (c) same as (a), for a lower modulation depth $\beta_A = 1.5$, $\beta_B = 0.5$. (d) Output P2 pattern from Ikeda map (solid curve) and LLE (dashed curve); red (blue) curves, even (odd) roundtrips.

ϕ_0), where pulse trains alternate in time between even and odd round-trips [see Fig. 1(d)], after the steady regime is reached.

Let us consider how the GVD modulation with the period equal to the cavity length ($N = 1$) alters the previous scenario. Figure 2 shows the parametric gain obtained from (a) the map, and (b) the LLE. We notice several important features: (i) the GVD periodicity enhances the gain and extends the P1 and P2 branches already present in the uniform cavity (compare Fig. 2(a) with Fig. 1(a)); (ii) Additional parametric MI bands appear, as clear from Fig. 2(a). These bands are alternating P1 (m even) and P2 (m odd) bands from left to right (as ω increases). The number of band increases (decreases) for large (weak) modulations, as revealed by the comparison between Fig. 2(a) and (c); (iii) the LLE gives a reliable picture for (even large) negative phase shifts (i.e., positive detunings δ), but still fails to describe the behavior for large $\phi_0 > 0$ (in particular close to antiresonance); (iv) In the LLE [Fig. 2(b)], the second branch, of P2 type, corresponding to $m = 1$ in Eq. (16) appears to be the natural continuation of the $m = 1$ branch of the map in Fig. 2(a). In particular, one can notice from Fig. 2(b) that for $\phi_0 < 0$, slightly increasing the value of $|\phi_0|$, one can switch from a situation where only the Faraday branch $m = 1$ is unstable to the regime where the latter coexist with the low frequency Turing branch, which is the regime experimentally investigated in [16]. This regime is well described by the LLE, as also witnessed by comparing the P2 pulse trains obtained for the map and the LLE, as shown in Fig. 2(d). It is worth pointing out that for the $m = 1$ branch (and similarly for $m = 3, 5, \dots$), the perturbation can grow up to steady-state shown in Fig. 2(d), exactly because it replicates in-phase after each pair of round-trips.

It is worth analyzing the effect of decreasing the GVD period to a fraction of the cavity length ($N \neq 1$). In this case, we calculate the eigenvalues and the region of instability numerically from the matrix (10). The relative gain is reported in Fig. 3 in the normalized frequency-power plane (ω, P) . In this plane, the low frequency branch stands for the Turing-type MI, which occurs on the lower branch of the bistable response, whereas the

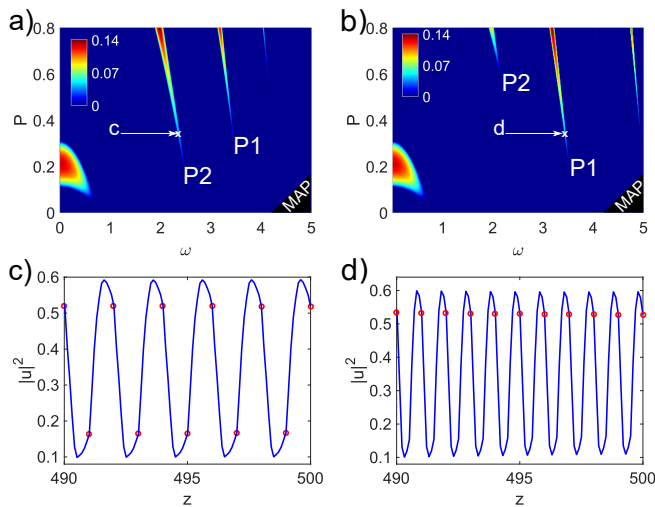


Fig. 3. (a) Color level plot of gain $g(\omega)$ for an inhomogeneous cavity with $\beta_A = 1.5$, $\beta_B = 0.5$ ($\Lambda = z_L = 1$ or $N = 1$), $z_A = z_B = 0.5$, $\phi_0 = -\pi/10$, $\alpha = \theta^2/2 = 0.05$. (b) Same as (a) for $z_A = z_B = 0.25$ ($\Lambda = z_L/2$ or $N = 2$). (c-d) Intracavity field evolution (blue curve) calculated from the map at $P = 0.35$ for (c) $\Lambda = 1$ and (d) $\Lambda = 1/2$. Red dots correspond to the observable field at the output coupler.

higher frequency branches occurs on the upper branch (higher power). By comparing the case $\Lambda = 1$ ($N = 1$) shown in Fig. 3(a) with the case $\Lambda = 1/2$ ($N = 2$) shown in Fig. 3(b), one notices that the halved period tends to enhance the P1 branch at the expense of the P2 branch. This fact is also illustrated in Figs. 3(c)-(d), which report the evolution of the intracavity field (blue curves) for fixed power and detuning for (c) $\Lambda = 1$ and (d) $\Lambda = 1/2$. The suppression of the P2 can be easily understood by considering that the P2 pattern is out-of-phase at each period. Given the fact that the cavity contains two periods, the output patterns will be in phase at the cavity output coupler at every round-trip. This justification holds strictly for the LLE model, where there is no trace left of the cavity period (MI gain map not shown). Conversely, for the map the cavity boundary conditions still play a role and can generate their own P2 branch at higher power (see Fig. 3(a)-(b)). To date the prevalence of P1 over P2 parametric (Faraday) instability lacks experimental confirmation. Clearly the prevalence of P1 MI branch for $N = 2$ holds in a range of small cavity phase-shifts. A comparison between the map and the LLE for this situation is displayed in Fig. 4 in the (ω, ϕ_0) plane. As shown, the LLE gives a good description of the phenomenon close to resonance $\phi_0 \simeq 0$, i.e. between horizontal dashed lines in Fig. 4.

In summary we have reported a unified matrix approach to study MI in passive cavities, both homogeneous or with piecewise constant built-in GVD, which allows to characterize the P1 and P2 regimes of MI. We unveiled the nature of Faraday instabilities in inhomogeneous cavities which have an odd number of GVD periods. Moreover, we highlighted the intrinsic limitations of the approach based on the LLE in view of correctly designing future experiments. Our analysis may suggest novel regimes for fiber-based frequency combs, which have been recently exploited as a compact and agile spectroscopic tool [29].

The present research was supported by IRCICA (USR 3380 CNRS), by the Labex CEMPI (ANR-11-LABX-0007-01), Equipex FLUX (ANR-11-EQPX-0017), by the projects NoAWE (ANR-14-

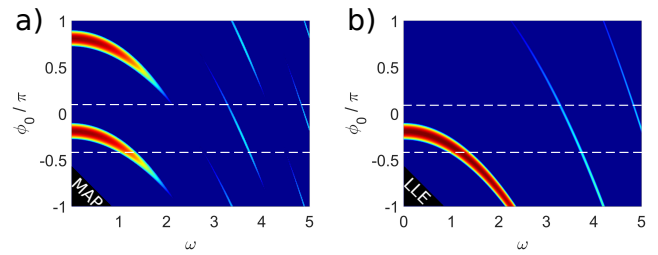


Fig. 4. Comparison of map (a) and LLE (b), as in Fig. 2(a,b), for an inhomogeneous cavity with $z_A = z_B = \Lambda/2 = 0.25$ ($N = 2$), and $\beta_A = 1.9$, $\beta_B = 0.1$, $P = 0.3$. The dashed horizontal lines delimit the region of validity of the LLE.

ACHN-0014), TOPWAVE (ANR-13-JS04-0004), CPER "Photonics for Society", and PRIN 2012BFNWZ2.

REFERENCES

1. K. Ikeda and O. Akimoto, *Phys. Rev. Lett.* **48**, 617–620 (1982).
2. H. Nakatsuka, S. Asaka, H. Itoh, K. Ikeda and M. Matsuoka, *Phys. Rev. Lett.* **50**, 109–112 (1983).
3. D. W. McLaughlin, J. V. Moloney, and A. C. Newell, *Phys. Rev. Lett.* **54**, 681 (1985).
4. L. A. Lugiato and R. Lefever, *Phys. Rev. Lett.* **58**, 2209 (1987).
5. M. Haelterman, S. Trillo, and S. Wabnitz, *Opt. Lett.* **17**, 745–747 (1992).
6. M. Haelterman, S. Trillo, and S. Wabnitz, *Opt. Commun.* **91**, 401–407 (1992).
7. S. Coen, H. G. Randle, T. Silvestre, and M. Erkintalo, *Opt. Lett.* **38**, 37–39 (2013).
8. F. Leo, A. Mussot, P. Kockaert, P. Emplit, M. Haelterman, and M. Taki, *Phys. Rev. Lett.* **110**, 104103 (2013).
9. P. Grelu *ed.*, *Nonlinear Optical Cavity Dynamics: From Microresonators to Fiber Lasers*, Wiley (2016).
10. M. Conforti, A. Mussot, A. Kudlinski, and S. Trillo, *Opt. Lett.* **39**, 4200–4203 (2014).
11. K. Staliunas, C. Hang, and V. V. Konotop, *Phys. Rev. A* **88**, 023846 (2013).
12. A. M. Perego, N. Tarasov, D. V. Churkin, S. K. Turitsyn, and K. Staliunas, *Phys. Rev. Lett.* **116**, 28701 (2016).
13. A. H. Nayfeh and D. T. Mook, *Nonlinear Oscillations* (Wiley, New York, 1979).
14. S. Rota Nodari, M. Conforti, G. Dujardin, A. Kudlinski, A. Mussot, S. Trillo, and S. De Bièvre, *Phys. Rev. A* **92**, 013810 (2015).
15. K. Staliunas, S. Longhi, and G. J. de Valcárcel, *Phys. Rev. Lett.* **89**, 210406 (2002).
16. F. Copie, M. Conforti, A. Kudlinski, A. Mussot, and S. Trillo, *Phys. Rev. Lett.* **116**, 143901 (2016).
17. F. Matera, A. Mecozzi, M. Romagnoli, and M. Settembre, *Opt. Lett.* **18**, 1499–1501 (1993).
18. J. Bronski and J. N. Kutz, *Opt. Lett.* **21**, 937–939 (1996).
19. N. J. Smith and N. J. Doran, *Opt. Lett.* **21**, 570–572 (1996).
20. F. Kh. Abdullaev and J. Garnier, *Phys. Rev. E* **60**, 1042–1050 (1999).
21. A. Armaroli and F. Biancalana, *Opt. Express* **20**, 25096–25110 (2012).
22. M. Droques, A. Kudlinski, G. Bouwmans, G. Martinelli, and A. Mussot, *Opt. Lett.* **37**, 4832–4834 (2012).
23. C. Finot, J. Fatome, A. Sysoliatin, A. Kosolapov, and S. Wabnitz, *Opt. Lett.* **38**, 5361–5364 (2013).
24. S. Coen and M. Haelterman, *Phys. Rev. Lett.* **21**, 4139–4142 (1997).
25. S. Coen and M. Haelterman, Ph. Emplit, L. Delage, L.M. Simohamed, and F. Reynaud, *J. Opt. Soc. Am. B* **15**, 2283 (1998).
26. D. A. Zezyulin, V. V. Konotop, and M. Taki, *Opt. Lett.* **36**, 4623 (2011).
27. T. Hansson and S. Wabnitz, *J. Opt. Soc. Am. B* **32**, 1259 (2015).
28. P. Del'Haye, A. Coillet, W. Loh, K. Beha, S. B. Papp, and S. A. Diddams, *Nature Comm.* **6**, 5668 (2015).
29. G. Millot, S. Pitois, M. Yang, T. Hovhannisyan, A. Bendamane, T. W. H. Hanch, and N. Picqué, *Nature Photon.* **10**, 27 (2016).

INFORMATIONAL FIFTH PAGE

REFERENCES

1. K. Ikeda and O. Akimoto, "Instability leading to periodic and chaotic self-pulsation in a bistable optical cavity", *Phys. Rev. Lett.* **48**, 617–620 (1982).
2. H. Nakatsuka, S. Asaka, H. Itoh, K. Ikeda and M. Matsuoka, "Observation of bifurcation to chaos in an all-optical bistable system", *Phys. Rev. Lett.* **50**, 109–112 (1983).
3. D. W. McLaughlin, J. V. Moloney, and A. C. Newell, "New class of instabilities in passive optical cavities", *Phys. Rev. Lett.* **54**, 681 (1985).
4. L. A. Lugiato and R. Lefever, "Spatial dissipative structures in passive optical systems", *Phys. Rev. Lett.* **58**, 2209 (1987).
5. M. Haelterman, S. Trillo, and S. Wabnitz, "Additive-modulation-instability ring fiber laser in the normal dispersion regime of a fiber," *Opt. Lett.* **17**, 745–747 (1992).
6. M. Haelterman, S. Trillo, and S. Wabnitz, "Dissipative modulation instability in a nonlinear dispersive ring cavity," *Opt. Commun.* **91**, 401–407 (1992).
7. S. Coen, H. G. Randle, T. Silvestre, and M. Erkintalo, "Modelling of octave-spanning Kerr frequency combs using a generalized mean-field Lugiato-Lefever model," *Opt. Lett.* **38**, 37–39 (2013).
8. F. Leo, A. Mussot, P. Kockaert, P. Emplit, M. Haelterman, and M. Taki, "Nonlinear symmetry breaking induced by third order dispersion in optical fiber cavities," *Phys. Rev. Lett.* **110**, 104103 (2013).
9. P. Grelu *ed.*, *Nonlinear Optical Cavity Dynamics: From Microresonators to Fiber Lasers*, Wiley (2016).
10. M. Conforti, A. Mussot, A. Kudlinski, and S. Trillo, "Modulational instability in dispersion oscillating fiber ring cavities", *Opt. Lett.* **39**, 4200–4203 (2014).
11. K. Staliunas, C. Hang, and V. V. Konotop, "Parametric patterns in optical fiber ring nonlinear resonators", *Phys. Rev. A* **88**, 023846 (2013).
12. A. M. Perego, N. Tarasov, D. V. Churkin, S. K. Turitsyn, and K. Staliunas, "Pattern generation by dissipative parametric instability", *Phys. Rev. Lett.* **116**, 28701 (2016).
13. A. H. Nayfeh and D. T. Mook, *Nonlinear Oscillations* (Wiley, New York, 1979).
14. S. Rota Nodari, M. Conforti, G. Dujardin, A. Kudlinski, A. Mussot, S. Trillo, and S. De Bièvre, "Modulational instability in dispersion-kicked optical fibers", *Phys. Rev. A* **92**, 013810 (2015).
15. K. Staliunas, S. Longhi, and G. J. de Valcárcel, "Faraday patterns in Bose-Einstein condensates", *Phys. Rev. Lett.* **89**, 210406 (2002).
16. F. Copie, M. Conforti, A. Kudlinski, A. Mussot, and S. Trillo, "Competing Turing and Faraday instabilities in dispersion oscillating passive resonators", *Phys. Rev. Lett.* **116**, 143901 (2016).
17. F. Matera, A. Mecozzi, M. Romagnoli, and M. Settembre, "Sideband instability induced by periodic power variation in long-distance fiber links," *Opt. Lett.* **18**, 1499–1501 (1993).
18. J. Bronski and J. N. Kutz, "Modulational stability of plane waves in nonreturn-to-zero communications systems with dispersion management," *Opt. Lett.* **21**, 937–939 (1996).
19. N. J. Smith and N. J. Doran, "Modulational instabilities in fibers with periodic dispersion management," *Opt. Lett.* **21**, 570–572 (1996).
20. F. Kh. Abdullaev and J. Garnier, "Modulational instability of electromagnetic waves in birefringent fibers with periodic and random dispersion," *Phys. Rev. E* **60**, 1042–1050 (1999).
21. A. Armaroli and F. Biancalana, "Tunable modulational instability sidebands via parametric resonance in periodically tapered optical fibers," *Opt. Express* **20**, 25096–25110 (2012).
22. M. Droques, A. Kudlinski, G. Bouwmans, G. Martinelli, and A. Mussot, "Experimental demonstration of modulation instability in an optical fiber with a periodic dispersion landscape," *Opt. Lett.* **37**, 4832–4834 (2012).
23. C. Finot, J. Fatome, A. Sysoliatin, A. Kosolapov, and S. Wabnitz, "Competing four-wave mixing processes in dispersion oscillating telecom fiber," *Opt. Lett.* **38**, 5361–5364 (2013).
24. S. Coen and M. Haelterman, "Modulational instability induced by cavity boundary conditions in a normally dispersive optical fiber," *Phys. Rev. Lett.* **21**, 4139–4142 (1997).
25. S. Coen and M. Haelterman, Ph. Emplit, L. Delage, L. M. Simohamed, and F. Reynaud, "Experimental investigation of the dynamics of a stabilized nonlinear fiber ring resonator," *J. Opt. Soc. Am. B* **15**, 2283 (1998).
26. D. A. Zezyulin, V. V. Konotop, and M. Taki, "Modulational instability in a passive fiber cavity, revisited", *Opt. Lett.* **36**, 4623 (2011).
27. T. Hansson and S. Wabnitz, "Frequency comb generation beyond the Lugiato-Lefever equation: multi-stability and super cavity solitons", *J. Opt. Soc. Am. B* **32**, 1259 (2015).
28. P. Del'Haye, A. Coillet, W. Loh, K. Beha, S. B. Papp, and S. A. Diddams, "Phase steps and resonator detuning measurements in microresonator frequency combs", *Nature Comm.* **6**, 5668 (2015).
29. G. Millot, S. Pitois, M. Yang, T. Hovhannisyann, A. Bendamane, T. W. Hansch, and N. Picqué, "Frequency-agile dual-comb spectroscopy", *Nature Photon.* **10**, 27 (2016).